Int J CARS (2016) 11:937–945
DOI 10.1007/s11548-016-1369-4

ORIGINAL ARTICLE

# Joint registration of ultrasound, CT and a shape+pose statistical model of the lumbar spine for guiding anesthesia

**Delaram Behnami[1] · Alexander Seitel[1] · Abtin Rasoulian[1] · Emran Mohammad Abu Anas[1] · Victoria Lessoway[2] · Jill Osborn[3] · Robert Rohling[1,4] · Purang Abolmaesumi[1]**

Received: 1 February 2016 / Accepted: 26 February 2016 / Published online: 16 March 2016


**Abstract**
*Purpose* Facet joint injections and epidural needle insertions are widely used for spine anesthesia. Accurate needle placement is important for effective therapy delivery and avoiding complications arising from damage of soft tissue and nerves. Needle guidance is usually performed by fluoroscopy or palpation, resulting in radiation exposure and multiple needle re-insertions. Several ultrasound (US)-based approaches have been proposed but have not found wide acceptance in clinical routine. This is mainly due to difficulties in interpretation of the complex spinal anatomy in US, which leads to clinicians' lack of confidence in relying only on information derived from US for needle guidance.
*Methods* We introduce a multimodal joint registration technique that takes advantage of easy-to-interpret preprocedure computed topography (CT) scans of the lumbar spine to concurrently register a shape+pose model to the intraprocedure 3D US. Common shape coefficients are assumed between two modalities, while pose coefficients are specific to each modality.
*Results* The joint method was evaluated on patient data consisting of ten pairs of US and CT scans of the lumbar spine. It was successfully applied in all cases and yielded an RMS shape error of 2.1 mm compared to the CT ground truth. The joint registration technique was compared to a previously proposed method of statistical model to US registration Rasoulian et al. (Information processing in computer-assisted interventions. Springer, Berlin, pp 51–60, 2013). The joint framework improved registration accuracy to US in 7 out of 17 visible vertebrae, belonging to four patients. In the remaining cases, the two methods were equally accurate.
*Conclusion* The joint registration allows visualization and augmentation of important anatomy in both the US and CT domain and improves the registration accuracy in both modalities. Observing the patient-specific model in the CT domain allows the clinicians to assess the local registration accuracy qualitatively, which is likely to increase their confidence in using the US model for deriving needle guidance decisions.

**Keywords** Multi-vertebrae model · Statistical shape+pose model · Spinal ultrasound · Joint registration · Guidance

## Introduction

Lumbar spine injections, including facet joint injections and epidural needle insertions, are widely used for delivering anesthesia and analgesia [2,4]. Facet joint injections are performed on patients suffering from lower back pain, a problem experienced at least once by 80 % of the adult population [19]. These procedures are particularly challenging due to the proximity to nerve tissue, the deep location of the target, the small and narrow size of the channel between the articular processes of the joint, and the oblique entry angle [2]. Hence, careful needle placement is of utter importance to ensure no damage is done to the nerves and nearby

✉ Delaram Behnami
delaramb@ece.ubc.ca

1 Department of Electrical and Computer Engineering, University of British Columbia, Vancouver, BC, Canada

2 Department of Ultrasound, Women's Hospital, Vancouver, BC, Canada

3 Department of Anesthesia, St. Paul's Hospital, Vancouver, BC, Canada

4 Department of Mechanical Engineering, University of British Columbia, Vancouver, BC, Canada

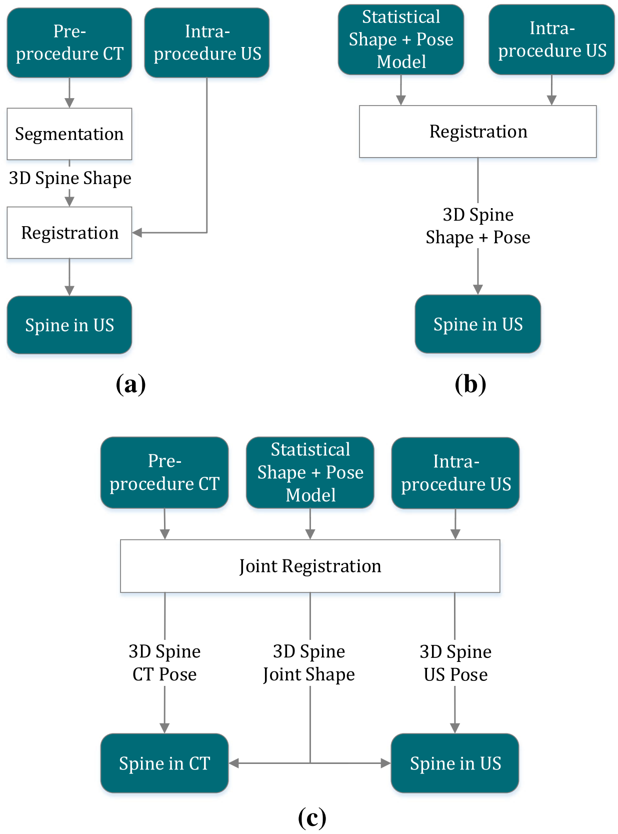


**Fig. 1** Overview of the state of the art for augmenting anatomical information with spinal US. Methods (**a**–**c**) are proposed by [3,5,10,13,17,18,23,24] and current paper, respectively

soft tissue, and the therapy is effective [25]. The current standard of care for these procedures is fluoroscopy, which imposes health risks due to exposure to ionizing radiation and requires specialized equipment [25]. Epidural needle insertions are also used to alleviate chronic pain [11]. In epidural anesthesia, needle insertion is done with the help of manual palpation and the loss-of-resistance technique [11]. In both facet joint and epidural injections, inaccurate needle placement can lead to complications such as accidental dural puncture (2.5 %, or 3–5 % for inexperienced operators) and post-puncture headache (86 %) [1,7,21]. Performing these procedures becomes even more challenging in the cases of obese patients, those suffering from scoliosis, and patients with previous back surgery [25].

Consequently, interest has increased in US as a non-ionizing, accessible, and inexpensive imaging modality [25]. Many studies indicate the feasibility of US guidance for spine interventions [6,12,15,22,25]. However, at present, none of these methods are clinically used due to challenges in interpreting the complex anatomy in spinal US images.

Most patients receiving routine injections for back pain have previous preprocedure images [such as computed topography (CT) or magnetic resonance (MR) images] available, since they were used for initial diagnosis [20]. Several methods have focused on registering these easy-to-interpret preprocedure images to the intraprocedure US [5,13,23,24] (Fig. 1a). These methods require an accurate segmentation of the vertebrae in the preprocedure data. Manual segmentation of CT or MR is very time consuming and labor intensive, and hence not practical for anesthesiologists or interventional radiologists in busy clinics. On the other hand, automatic segmentation of preprocedure data for accurate intraoperative registration to US within the operation time has been proven challenging. Furthermore, even in the presence of accurate segmentation of the spine from the preprocedure CT or MR data, clinically, the fields-of-view of preprocedure data is normally limited (mostly to limit radiation dose in CT or reduce acquisition time in MR), covering only a portion of the anatomy that is imaged during the procedure for targeting.

To overcome these issues, our group has proposed several methods to register a statistical shape model of the lumbar spine to the US [10,17] (Fig. 1b). Rasoulian et al. [18] proposed to improve guidance accuracy using a statistical multi-vertebrae shape+pose model for tracked 2D US. Brudfors et al. [3] investigated registering a similar shape+pose model to tracker-less 3D US. While these methods are promising, model to US registration errors vary in magnitude and location. Therefore, there is need to improve and assess the accuracy of the specific model generated for each patient, and to provide the clinician with additional confidence for the accuracy of intraprocedure augmentation.

In this paper, we propose an approach that jointly registers a statistical shape+pose model of the spine to limited field-of-view preprocedure images from CT and intraprocedure US (Fig. 1c). Our aim is multimodal registration and visualization of the model on both domains, as well as to enable visualization of the model, while attempting to improve US interpretation for facet joint and epidural injections by taking advantage of available preprocedure CT. The rest of this paper is organized as follows. In "Materials and methods" section, we provide an overview of the methods and materials used for joint multimodal registration. In "Results" section, we report the results, and in "Discussion and conclusion" section, we discuss and conclude the paper.

## Materials and methods

Figure 2 shows an overview of the joint registration approach. The main idea is to use preoperative imaging information to improve a model-based registration in 3D US volumes. Central to the method is the underlying shape+pose model of the lumbar spine ("Statistical multi-object shape+pose model of the lumbar spine" section). For both US and CT data, a point cloud representing the bone surfaces is extracted ("Target

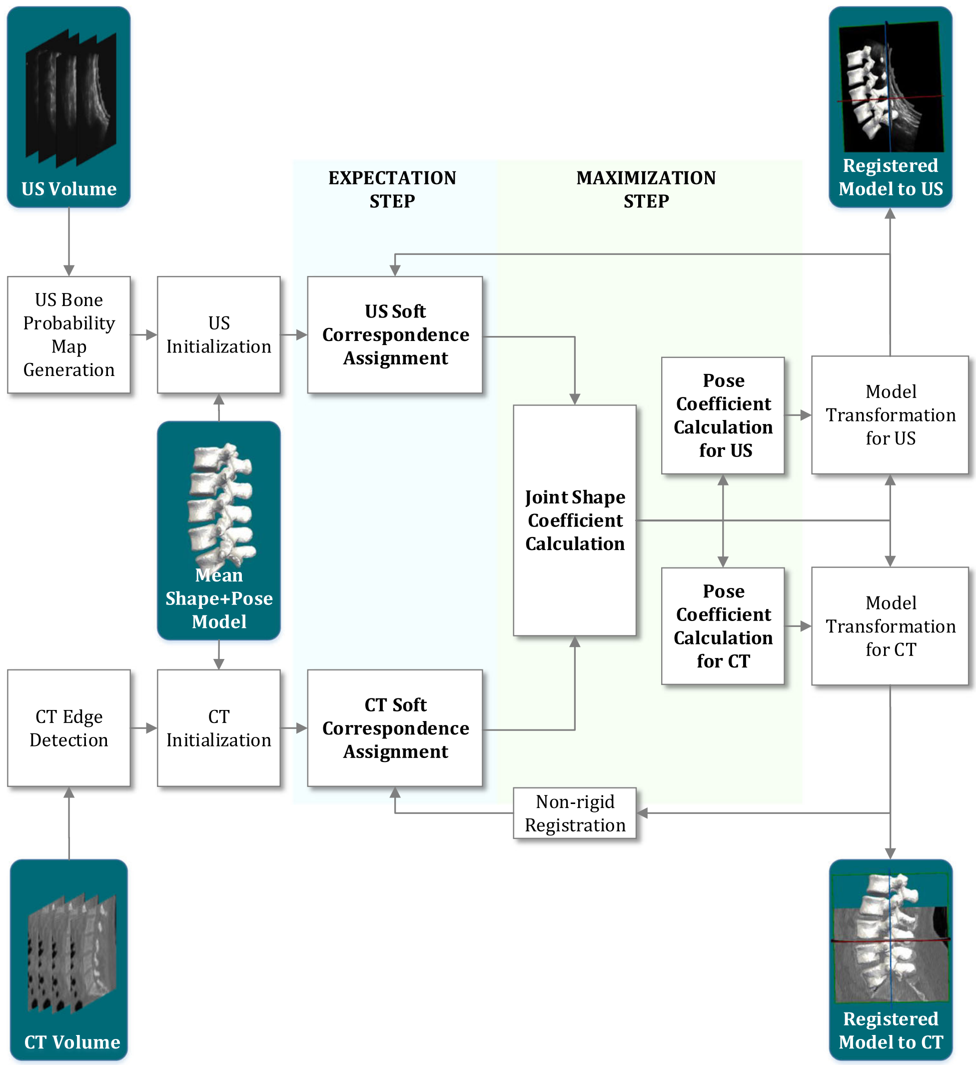


**Fig. 2** Overview of the proposed framework for joint registration of US, CT and a statistical shape+pose model

point cloud generation" section) and the model is approximately initialized within the volume ("Model initialization" section). Finally, the shape and pose coefficients of the model are jointly optimized ("Joint optimization and registration" section) such that the model can be overlaid in both US and CT space.

## Statistical multi-object shape+pose model of the lumbar spine

We base our approach on the statistical shape+pose model of the lumbar spine and its registration to CT and US images as presented in our previous work [16]. The model is generated from 32 segmented CT images obtained in an independent study. The model can be instantiated by applying different weights to the principal components (PC) determined during model training and combining them. Assuming that $\theta_k^{\mathrm{s}}$ is the coefficient applied to the $k$th shape PC and $\theta_k^{\mathrm{p}}$ is the coefficient applied to the $k$th pose PC, the $l$th object of the model can be instantiated as follows:

$$\Phi(\theta^{\mathrm{s}}, \theta^{\mathrm{p}}) = \Phi_l^{\mathrm{p}}\left(\Phi_l^{\mathrm{s}}(\theta^{\mathrm{s}}); \theta^{\mathrm{p}}\right), \qquad (1)$$

where $\Phi_l^{\mathrm{p}}(\cdot; \theta^{\mathrm{p}})$ represents a similarity transformation built as a weighted combination of the pose PCs and $\Phi_l^{\mathrm{s}}(\cdot)$ describes the associated shape instantiation.

## Target point cloud generation

To allow for an accurate registration of the statistical model to both the CT and the US volume, the bone surface has to be extracted in both modalities.

For the CT volume, a point cloud is obtained from the visible edges of the lumbar spine. Edges are extracted using a simple Canny edge detector [16].

The US volume is preprocessed by applying a phase-based bone enhancement technique [9] that results in a so-called bone probability map indicating how probable each voxel of the volume represents bone tissue. The enhanced volume is then thresholded, yielding a probabilistic point cloud, where the probabilities are used for the soft correspondence assignment.

### Model initialization

To avoid the registration converging far off the optimal solution, the model has to be aligned roughly at the correct anatomical position. In most cases, the assumption can be made that CT is acquired in supine position, while US volumes are acquired with the patient in prone position. This allows us to apply a simple one-click landmark-based initialization approach where the approximate center of gravity of the L3 vertebra is defined in US/CT space and the model is translated accordingly. In the case of CT initialization, a rigid registration is then performed to further improve the initial alignment.

### Joint optimization and registration

In our previous works [16,18], registration of the statistical shape+pose model to a target point cloud extracted from the volume acquired by a single modality (e.g., US or CT) is accomplished by optimizing the model parameters using the expectation-maximization (EM) algorithm. In the expectation step, we compute the probabilities of each $n$th model point belonging to the $l$th object ($t_n^l$) generating a target point $z_m$. For imaging modalities such as CT and MR, $z_m$'s are all equally weighted, whereas in the case of US, they are assigned probabilities indicating how likely it is for each point to represent bone. $P({t_n}^l|z_m)$ can be calculated as we described before [16]. In the maximization step, the following objective function is optimized.

$$Q = \sum_{l=1}^{L} \sum_{m,n=1}^{M,N_l} P({t_n}^l|z_m)||z_m - \Phi\left(t_n^l, \theta^{\mathrm{s}}, \theta^{\mathrm{p}}\right)||^2 + R^{\mathrm{s}} + R^{\mathrm{p}} \tag{2}$$

where $\Phi(t_n^l, \theta^{\mathrm{s}}, \theta^{\mathrm{p}})$ denotes the transformation of point $t_n^l$ on the model with the shape and pose coefficients $\theta^{\mathrm{s}}$ and $\theta^{\mathrm{p}}$. $M$ and $N$ represent the number of points on the model and image, respectively. The regularizers $R^{\mathrm{s}}$ and $R^{\mathrm{p}}$ constrain the shape and pose variations, respectively, and are computed according to [16].

In this work, in order to incorporate information from more than one modality, the objective function is chosen as the sum of distances from the points in the model to the data points coming from both modalities of interest, namely CT and US. The shape of the vertebrae remains the same before and during the procedure for each individual patient. The pose of the individual vertebrae, on the other hand, will change between preprocedure CT and intraoperative US imaging. Let $md \in \{\mathrm{US, CT}\}$ denote the target's imaging modality. $z_{m,md}$ will then represent the $m$th point from the point cloud (size $M_{md}$) of each given modality. Therefore, $\Phi(t_n^l, \theta^{\mathrm{s}}, \theta^{\mathrm{p}}_{md})$ represents the transformation of model points $t_n^l$ with the common shape coefficients $\theta^{\mathrm{s}}$ and the individual modality-specific pose coefficients $\theta^{\mathrm{p}}_{md}$. To sum over distances from the transformed model to the target points of both modalities, we extend the objective function to the following:

$$Q = \sum_{md \in \{\mathrm{US,\ CT}\}} \sum_{l=1}^{L} \sum_{m,n=1}^{M_{md},N_l} P({t_n}^l|z_{m,md})||z_{m,md} - \Phi\left(t_n^l, \theta^{\mathrm{s}}, \theta^{\mathrm{p}}_{md}\right)||^2 + R^{\mathrm{s}} + R^{\mathrm{p}}_{md}. \tag{3}$$

The above equation holds for any subset $\mathrm{MD} \subseteq \{\mathrm{US, CT}\}$; $\mathrm{MD} \neq \emptyset$. Differentiating Eq. (3) with respect to the common shape coefficients gives:

$$\frac{\partial Q}{\partial \theta^{\mathrm{s}}} = \sum_{md \in \{\mathrm{US,\ CT}\}} \sum_{l=1}^{L} \sum_{m,n=1}^{M_{md},N_l} P({t_n}^l|z_{m,md}) \times \left[\Phi(t_n^l)^\top - {z_{m,md}}^\top \frac{\partial \Phi(t_n^l)}{\partial \theta_{\mathrm{s}}}\right] + R^{\mathrm{s}}. \tag{4}$$

Differentiation with respect to each set of pose coefficients $\theta^{\mathrm{p}}$ can be done in a similar fashion, yielding to the expression below:

$$\frac{\partial Q}{\partial \theta^{\mathrm{p}}_{md}} = \sum_{md \in \{\mathrm{US,\ CT}\}} \sum_{l=1}^{L} \sum_{m,n=1}^{M_{md},N_l} P\left({t_n}^l|z_m\right) \times \left[\Phi(t_n^l)^\top - {z_m}^\top \frac{\partial \Phi\left(t_n^l\right)}{\partial \theta_{\mathrm{p}}}\right] + R^{\mathrm{p}}_{md}. \tag{5}$$

Calculation of partial derivatives $\frac{\partial \Phi(t_n^l)}{\partial \theta_{\mathrm{s}}}$ and $\frac{\partial \Phi(t_n^l)}{\partial \theta_{\mathrm{p}}}$ has been previously presented in [16].

The EM-based algorithm used to register the point clouds is the coherent point drift [14]. In each iteration, the shape coefficients are jointly computed from both modalities. Subsequently, the pose coefficients are calculated from the shape coefficients separately for each modality.

### Validation

We validate our joint registration approach on ten patients whose spinal volumetric US data and corresponding CT data were available. US volume acquisition was performed with an electromagnetically tracked US probe [18]. For choosing the number of principal components for the CT pose and the joint shape, a separate set of ten segmented, publicly available CT data sets [8] were used and an exhaustive parameter search was performed with respect to the surface distance error (SDE). The number of principal components for the US pose was chosen according to [18]. The US-related parameters are set according to prior work by Hacihaliloglu et al. [9]. We evaluate the joint model registration quantitatively in the CT and US domain, as well as qualitatively in the US domain.

*Analysis in CT domain*

For each patient, the registered model is projected to the CT space which serves as a reference. The gold standard is obtained by manually segmenting the fully visible vertebrae each CT scan. For each visible vertebra in the CT volume, the shape SDE is computed between the registered model surface and the surface obtained from the gold standard. This error is calculated as the Euclidean distance between the points on one surface to their closest neighboring points on the other. In order to investigate only the shape errors, we rigidly register the estimated model surface at each vertebra with the gold standard surface manually segmented from the CT volume. This step eliminates potential pose errors when comparing to ground truth. In order to obtain a more thorough and detailed analysis of the results, the shape errors are reported at several regions: the spinous processes (SP), transverse processes (TP), anterior and posterior articular processes (AP) and vertebral bodies (VB). This breakdown is performed by manually selecting these regions on the gold standard on each vertebra, for each patient.

*Analysis in US domain*

In the US domain, we report differences in maximum SDE values obtained from the two models at the SP, measured by a sonographer. The maximum errors between each model and the visible SP are measured on anterior–posterior and inferior–superior planes, from the overlaid models (atlas-to-US and jointly registered models) to the US volumes. In addition to this quantitative analysis, based on the measured errors and the visual overlays, the sonographer was asked to decide which of the two registered model best matched the visible anatomical features. The two models are reported equal where the maximum differences between the errors are not easily visible, i.e., below 0.5 mm at each point, as well as cases where the net difference between the two models at the SP surface appears almost zero to the sonographer.

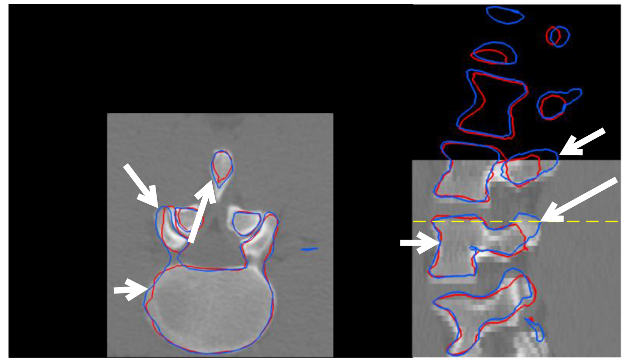

**Fig. 3** Example snapshot of US-to-atlas (*red*) and jointly registered (*blue*) models overlaid on corresponding CT scans for patient 5. The *yellow dashed line marks* the location of axial slice (*left*) in the sagittal view (*right*). The *white arrows* indicate regions where the joint registration is more accurate than the US-to-atlas registration

## Results

With the joint registration approach, we were able to achieve an overall RMS SDE of 2.1 mm and maximum SDE of 9.7 mm compared to the CT ground truth (SDE for US-only registration was 2.3 mm RMS and 11.3 mm at maximum). We analyzed the performance of the joint registration in both CT and US domains, while comparing and contrasting it with the US-only registration method. Sample snapshots of the overlay of the two models onto a CT scan and several US volumes are shown in Figs. 3 and 4, respectively.

Figure 5 shows the SDE differences in the two methods at different regions of the vertebrae, namely SP, TP, AP and VB. The joint approach leads to an overall improvement in the maximum and RMS errors for 8 out of 10 patients in CT space. Major improvements were observed at the SP region. Figure 6 shows the differences between the joint and the US-only registration as a colormap on the individual vertebrae for each of the ten patients. In Fig. 7, we provide the differences in maximum SDE from the SP in the US to either of the two registered models. These differences were measured by the expert sonographer at the SP of all vertebrae whose SPs were fully visible. According to the sonographer, based on error measurements and qualitative analysis, the joint model improved the registration accuracy in seven out of 17 vertebrae with visible SPs, belonging to four different patients. The two methods performed equally well in the remaining ten visible vertebrae. The sonographer was not able to locate the SPs in the vertebrae for the other six patients.

## Discussion and conclusion

In this paper, we presented a framework for joint registration of a statistical model of the lumbar spine to US and CT with

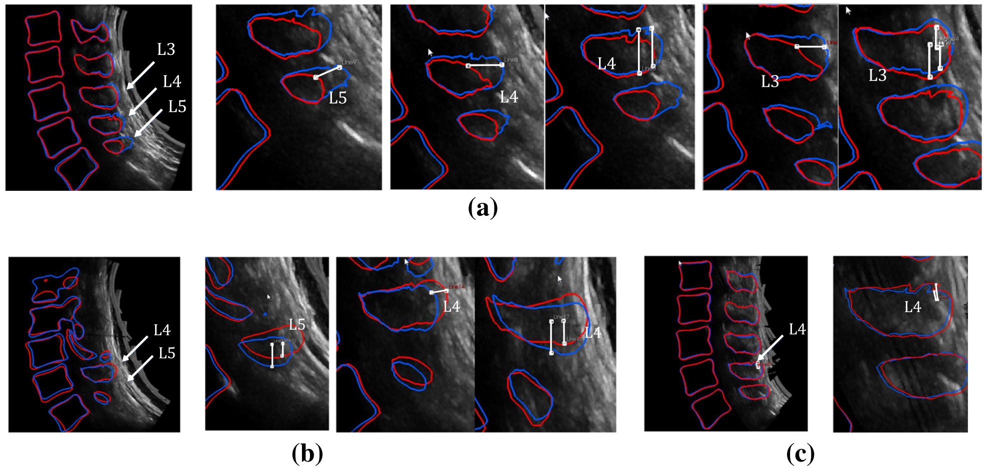


**Fig. 4** Snapshots of US-to-atlas (*red*) and jointly registered (*blue*) models overlaid on corresponding US volumes for patients 1 (**a**), 2 (**b**) and 6 (**c**). For each subfigure, the image on the *left* shows a sagittal view of the a full models, while close-ups of the SP regions are given on the *right* with marked measurements

**Fig. 5** Maximum SDE differences between the US-only and jointly registered models at regions SP, TP, AP and VB for all ten patients. The *positive bars* (*blue*) represent the amount of improvement obtained by using the joint method, while the *negative bars* (*red*) show decreased accuracy using the joint method. The individual errors are computed from each model to CT gold standard and averaged over all visible vertebrae for each patient

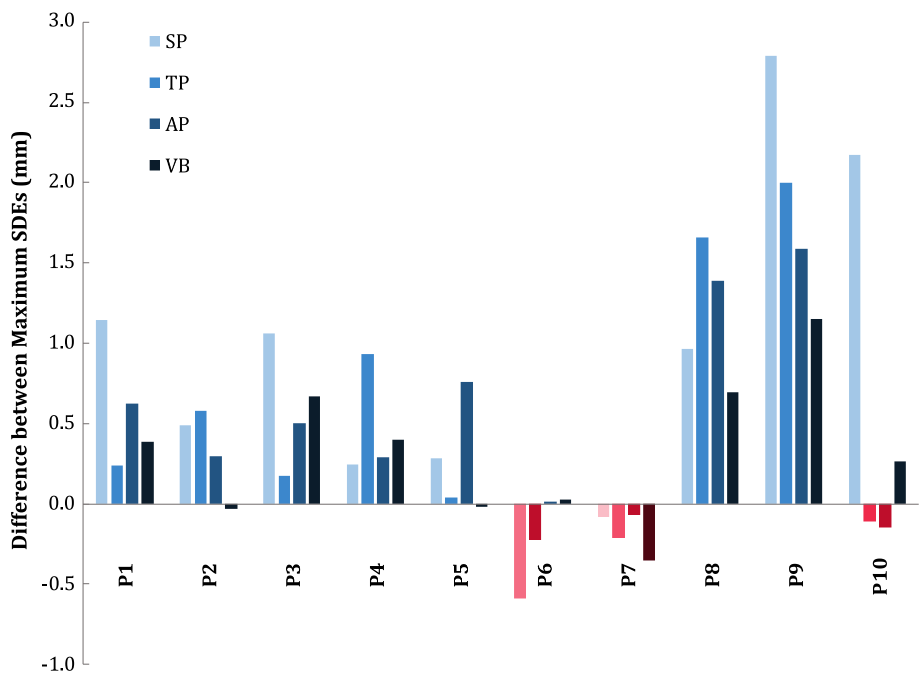


the aim to improve interpretation of the anatomy in spinal US for facet joint injections and epidural needle insertions. In our method, as a by-product of the joint registration, the pose coefficients of the spine in the CT domain are calculated (Fig. 2). This allows the model to be transformed and overlaid onto the CT domain, helping the clinician to qualitatively evaluate the local registration accuracy of the patient-specific model constructed for the US image based on the detailed anatomy visible in the CT scan. Hence, we showed that by including preprocedure CT, we allow for a simultaneous visualization of the spine anatomy in both US and CT domains without the need for preoperative segmentation of CT. Moreover, we demonstrated that by taking advantage of available easy-to-interpret preprocedure CT data for computing the shape of the statistical model, improved performance of the US registration can be achieved. The joint registration allowed a more accurate overlay of the anatomical information of the lumbar spine in both CT and US domain compared to the approach where only US information was used for registration.

Although results are improved by joint registration, individual cases show that errors in certain anatomical regions can still be decreased. We noticed that the registration accuracy of our joint model in more complicated areas of the

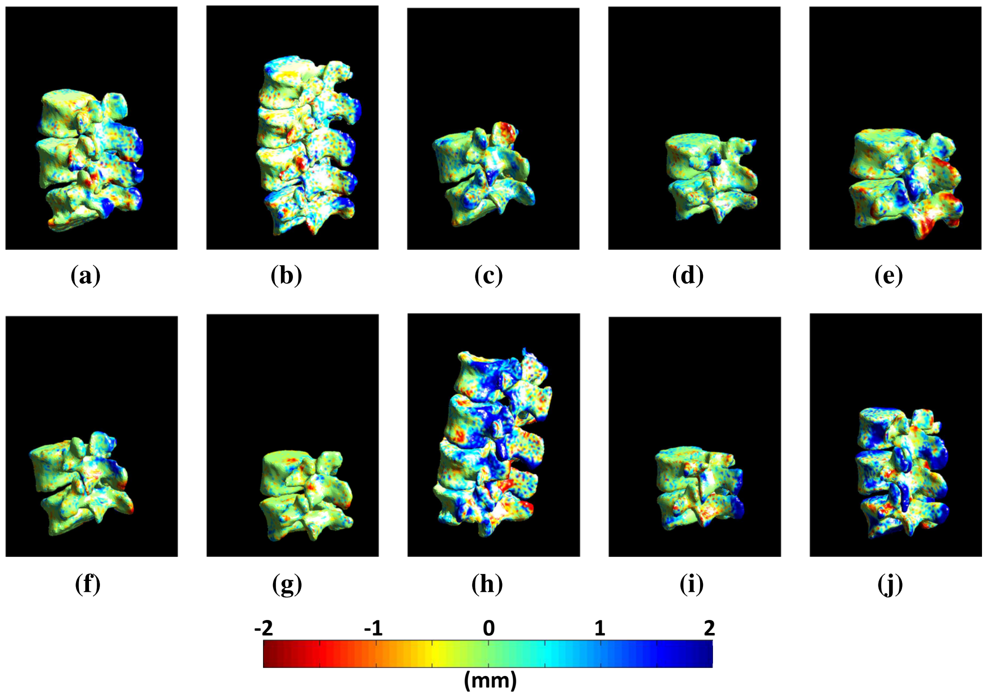


**Fig. 6** Colormaps showing the difference between shape SDE values per surface point computed from US-to-atlas and joint registrations, using segmented reference CT as the gold standard for patients 1 (**a**) to 10 (**j**). *Blue regions* show improvements achieved by the joint registration, where US-to-atlas error is larger than joint registration error

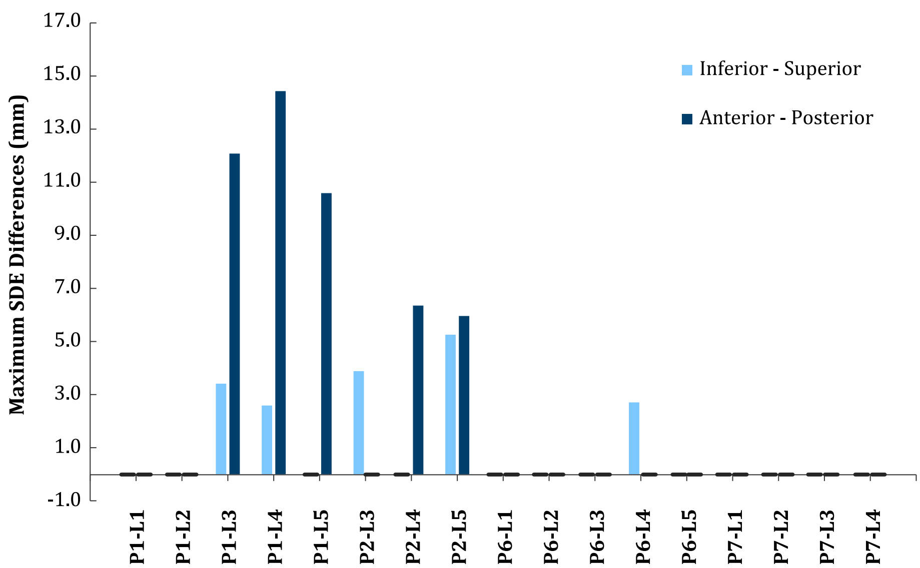


**Fig. 7** Difference between maximum SDE values of US-only model to US and jointly registered model to US at the SP of all vertebrae whose SPs are fully visible to the sonographer. The horizontal axis is labeled with the patient (P) and vertebra (L) number. Positive SDE values indicate higher errors for US-only model to US, i.e., improvement achieved using joint registration. Zero differences (*black dashes*) imply approximately equal accuracy. The *light blue bars* show improvements achieved by the joint method in the inferior–superior errors measured on transverse planes, while *dark blue bars* show the improvements in anterior–posterior distances measured on coronal planes

processes was not high enough in the CT domain which propagated to an apparently higher error in the US domain. We speculate that this issue stems from having a small size of training set (32 patients) used to generated the statistical spine model. Enlarging the training set can potentially lead to better results. Furthermore, correct edge detection for point cloud extraction in CT scans strongly depends on the quality and resolution of these image. As the examined CT volumes originate from routine clinical acquisitions with inhomogeneous voxel resolution, the bone surface is not sharply visible in all imaging axes, making it difficult to obtain a dense bone point cloud ideal for model registration. Improving CT image quality during acquisition or enhancing bone surface detection might further increase the registration accuracy.

The statistical spine model used in this study has been designed for the five lumbar vertebrae, with different pose and shape variations changing the entire structure as a whole. However, the CT scans used for testing the method included variable fields-of-view with two to four visible vertebrae. Only small improvements or even worsening of error values for patients 6 and 7 could be due to the fact that only two vertebrae were visible in their CT scans. For patients 1, 2, and 8–10, whose CT scans included three or four vertebrae, improvements were more pronounced. However, this problem is only observed in the CT domain, since according to our qualitative analysis, both registration methods seemed to perform equally well for cases 6 and 7 in the US domain.

All prior art involving statistical models for spine augmentation has been published by our group. Hence, in this paper, we simply evaluate our method in terms of SDE improvements (differences) achieved using the joint framework, as opposed to the US-only one (presented in [17]). While the previous methods also achieves good registration results, none allow for a simultaneous visualization of the spine anatomy in both US and CT domains without the need for preoperative segmentation of CT.

Future work can involve a user study, where sonographers will be asked to rate and comment on the effectiveness and viability of the presented framework for spinal ultrasound augmentation. Also, in this study, CT was the only preoperative modality that was investigated. The presented method could be generalized to magnetic resonance (MR) images as the preoperative modality. The same framework could also be used for joint registration to both CT and MR scans together with the statistical shape+pose model and US. We envision that such a multi-data fusion could further improve the final registration accuracy which, in turn, could further increase the confidence of the physician in using the these patient-specific models for making guidance decisions in spine anesthesia.

#### Compliance with ethical standards

**Conflict of interest** The authors declare that they have no conflicts of interest

**Human and animal rights** No new patient data were acquired for this work by any of the authors. This work does not contain any studies with animals.

## References

1. Abdi S, Datta S, Lucas LF (2005) Role of epidural steroids in the management of chronic spinal pain: a systematic review of effectiveness and complications. Pain Phys 8(1):127–43
2. Boswell MV, Colson JD, Spillane WF (2005) Therapeutic facet joint interventions in chronic spinal pain: a systematic review of effectiveness and complications. Pain Phys 8(1):101–114
3. Brudfors M, Seitel A, Rasoulian A, Lasso A, Lessoway VA, Osborn J, Maki A, Rohling RN, Abolmaesumi P (2015) Towards real-time, tracker-less 3D ultrasound guidance for spine anaesthesia. Int J Comput Assist Radiol Surg 10(6):855–865
4. Center P, Covington L, Parr A (2009) Lumbar interlaminar epidural injections in managing chronic low back and lower extremity pain: a systematic review. Pain Phys 12(1):163–188
5. Chen EC, Mousavi P, Gill S, Fichtinger G, Abolmaesumi P (2010) Ultrasound guided spine needle insertion. In: SPIE Medical Imaging. International Society for Optics and Photonics, pp 762,538–762,538
6. Conroy PH, Luyet C, McCartney CJ, McHardy PG (2013) Real-time ultrasound-guided spinal anaesthesia: a prospective observational study of a new approach. Anesthesiol Res Pract 2013:525818. doi:10.1155/2013/525818
7. de Oliveira Filho GR (2002) The construction of learning curves for basic skills in anesthetic procedures: an application for the cumulative sum method. Anesth Analg 95(2):411–416
8. Glocker B, Zikic D, Konukoglu E, Haynor DR, Criminisi A (2013) Vertebrae localization in pathological spine CT via dense classification from sparse annotations. In: MICCAI 2013—16th international conference on medical image computing and computer assisted intervention. Springer, Berlin. http://research.microsoft.com/apps/pubs/default.aspx?id=192918
9. Hacihaliloglu I, Rasoulian A, Rohling RN, Abolmaesumi P (2013) Statistical shape model to 3D ultrasound registration for spine interventions using enhanced local phase features. In: Medical image computing and computer-assisted intervention—MICCAI 2013. Springer, Berlin, pp 361–368
10. Khallaghi S, Mousavi P, Gong RH, Gill S, Boisvert J, Fichtinger G, Pichora D, Borschneck D, Abolmaesumi P (2010) Registration of a statistical shape model of the lumbar spine to 3D ultrasound images. In: Medical image computing and computer-assisted intervention—MICCAI 2010. Springer, Berlin, pp 68–75
11. Liu SS, Strodtbeck WM, Richman JM, Wu CL (2005) A comparison of regional versus general anesthesia for ambulatory anesthesia: a meta-analysis of randomized controlled trials. Anesth Analg 101(6):1634–1642
12. Loizides A, Peer S, Plaikner M, Spiss V, Galiano K, Obernauer J, Gruber H (2011) Ultrasound-guided injections in the lumbar spine. Med Ultrason 13(1):54–8
13. Moore J, Clarke C, Bainbridge D, Wedlake C, Wiles A, Pace D, Peters T (2009) Image guidance for spinal facet injections using tracked ultrasound. In: Medical image computing and computer-assisted intervention—MICCAI 2009. Springer, Berlin, pp 516–523
14. Myronenko A, Song X (2010) Point set registration: coherent point drift. IEEE Trans Pattern Anal Mach Intell 32(12):2262–2275
15. Niazi A, Chin K, Jin R, Chan V (2014) Real-time ultrasound-guided spinal anesthesia using the SonixGPS ultrasound guidance system: a feasibility study. Acta Anaesthesiol Scand 58(7):875–881
16. Rasoulian A, Rohling R, Abolmaesumi P (2013) Lumbar spine segmentation using a statistical multi-vertebrae anatomical shape+pose model. IEEE Trans Med Imaging 32(10):1890–1900
17. Rasoulian A, Rohling RN, Abolmaesumi P (2013) Augmentation of paramedian 3D ultrasound images of the spine. In: Information

processing in computer-assisted interventions. Springer, Berlin, pp 51–60

18. Rasoulian A, Seitel A, Osborn J, Sojoudi S, Nouranian S, Lessoway VA, Rohling RN, Abolmaesumi P (2015) Ultrasound-guided spinal injections: a feasibility study of a guidance system. Int J Comput Assist Radiol Surg 10(9):1417–1425
19. Rubin DI (2007) Epidemiology and risk factors for spine pain. Neurol Clin 25(2):353–371
20. Silbergleit R, Mehta BA, Sanders WP, Talati SJ (2001) Imaging-guided injection techniques with fluoroscopy and ct for spinal pain management 1. Radiographics 21(4):927–939
21. Sprigge J, Harper S (2008) Accidental dural puncture and post dural puncture headache in obstetric anaesthesia: presentation and management: a 23-year survey in a district general hospital. Anaesthesia 63(1):36–43
22. Tran D, Kamani AA, Al-Attas E, Lessoway VA, Massey S, Rohling RN (2010) Single-operator real-time ultrasound-guidance to aim and insert a lumbar epidural needle. Can J Anesth 57(4):313–321
23. Ungi T, Abolmaesumi P, Jalal R, Welch M, Ayukawa I, Nagpal S, Lasso A, Jaeger M, Borschneck DP, Fichtinger G, Mousavi P (2012) Spinal needle navigation by tracked ultrasound snapshots. IEEE Trans Biomed Eng 59(10):2766–2772
24. Yan CX, Goulet B, Pelletier J, Chen SJS, Tampieri D, Collins DL (2011) Towards accurate, robust and practical ultrasound-CT registration of vertebrae for image-guided spine surgery. Int J Comput Assist Radiol Surg 6(4):523–537
25. Yoon SH, O'Brien SL, Tran M (2013) Ultrasound guided spine injections: advancement over fluoroscopic guidance? Curr Phys Med Rehabil Rep 1(2):104–113